Atropisomeric Transition State Analogs

Olaf Ritzeler,[a][+] Serge Parel,[a] Bruno Therrien,[a] Nicolas Bensel,[a] Jean-Louis Reymond,*[a] and Kurt Schenk[b]

Keywords: Atropisomerism / Transition states / Enzyme inhibitors

Transition state mimicry is one of the most powerful concepts in enzyme inhibitor design and has led to the development of catalytic antibodies. Transition state analogs are compounds with a fixed shape that resemble the geometry and charge distribution of the transition state of a given reaction. Stabilization of a transition state like conformation is most often achieved by incorporating a ring system into the analog. We show herein that atropisomerism can be used as a new principle for enforcing a transition state like conformation. Atropisomerism relates to the existence of stereoisomers of structurally constrained molecules due to a frozen rotation about a single bond, as for example in binaphthol. The 1-aminomethylnaphthalene derivative **1** exhibits atropisomerism due to a frozen rotation about the C(1)–C(methylene) single bond, which holds the dihedral angle θ[C(2)–C(1)–C(methylene)–N] close to 90°. Compound **1** mimics the transition state for hydride transfer between 1,4-dihydroquinolines **4** and acetone.

Introduction

As first formulated by Pauling,[1] chemical catalysis may be described as tight binding between a catalyst and the transition state of a reaction.[2] This simple concept led to the development of transition state mimicry as a powerful paradigm in enzyme inhibitor design, as well as to the development of catalytic antibodies, whereby stable transition state analogs of chemical reactions are used in the creation of new catalytic activity through immunization.[3,4]

A transition state is defined as a saddle point on the Born–Oppenheimer hypersurface of a molecular system.[5] Transition state analogs are compounds with a fixed shape that resemble the geometry and charge distribution of a given transition state.[6] The construction of such stable analogs is generally difficult because transition state bond lengths and geometries are inherently unstable owing to their transient nature. Indeed, wherever possible one chooses to mimic not the transition state itself but a high energy intermediate along the reaction pathway, if such an intermediate exists. This approach includes the use of phosphonates as stable analogs of the tetrahedral intermediate in ester hydrolysis, and of polyhydroxylated five- and six-membered ring compounds as analogs of the oxocarbonium cation intermediate in glycosidic bond hydrolysis.[7]

Construction of a transition state analog almost always requires the fixing of a reactive conformation and/or a relative arrangement of reactants corresponding to the transition state. The strategy most often used to represent such conformations has been to incorporate ring systems in the transition state analog. Thus, five- and six-membered rings have been used to generate transition state analogs for the rearrangement of peptide bonds,[8] epoxy alcohol[9] and carbocationic cyclizations,[10] for pericyclic reactions such as oxy-Cope[11] rearrangements, selenoxide[12] and Cope[13] eliminations, and for alkene[14] and bis(aryl)[15] isomerization reactions. Similarly, bicyclic compounds have been used to mimic transition state conformations for Claisen rearrangements,[16] Diels–Alder cycloadditions,[17] a disfavored *Z*-selective β-fluoro-elimination,[18] and for glycosidic bond cleavage.[19] An α-keto-amide has been used to mimic the transition state for *cis–trans* isomerization in prolyl-peptide bonds.[20]

We report herein on a new principle for enforcing a transition state like conformation in a stable analog, namely the use of atropisomerism. Atropisomerism relates to the existence of stereoisomers of structurally constrained molecules due to a frozen rotation about a single bond, as for example in binaphthol.[21] Atropisomerism has provided the basis for the design of a number of highly enantioselective reagents and catalysts.[22] We show here that atropisomerism allows the design of transition state analogs for hydride transfer between a 1,4-dihydroquinoline and a methyl ketone. The transition state of this reaction is accurately mimicked using *N*-oxide model compounds.

Results and Discussion

Alcohol dehydrogenases are extremely important enzymes that catalyze reversible hydride transfer between the 4-position of a 1,4-dihydronicotinamide of an NADH (reduced nicotinamide adenine dinucleotide) or NADPH (reduced nicotinamide adenine dinucleotide phosphate) cofactor and the carbonyl group of an aldehyde or ketone

[a] Department of Chemistry and Biochemistry, University of Bern,
Freiestrasse 3, CH-3012 Bern, Switzerland
[b] Laboratoire de Cristallographie, BSP-Dorigny, Université de Lausanne,
CH-1015 Lausanne, Switzerland
[+] Present address: Hoechst Marion Roussel Deutschland GmbH, D-65926 Frankfurt, Germany

  1434–193X/00/0407–1365 $ 17.50+.50/0

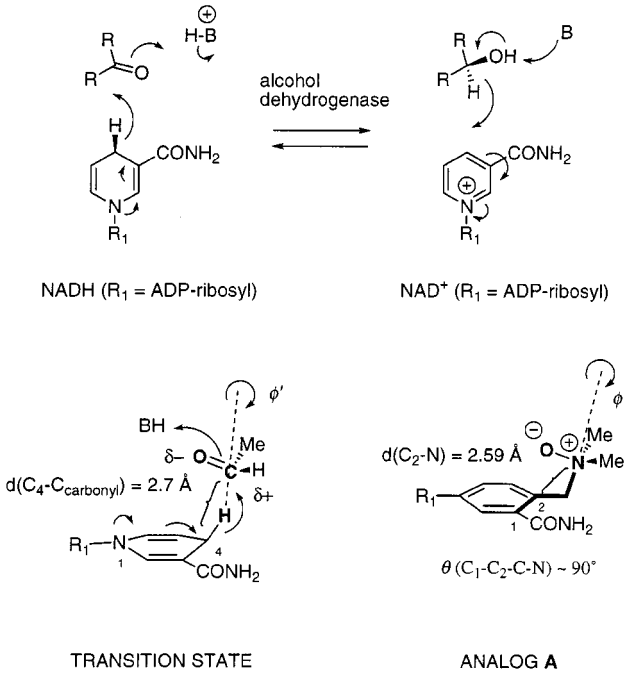

Scheme 1. Transition state and analogs for the alcohol dehydrogenase reaction

(Scheme 1).[23] The origin of this catalysis and the geometry of the transition state have been the subject of intense scientific debate in recent years. We have therefore become interested in preparing an alcohol dehydrogenase catalytic antibody. This requires the design of a stable transition state analog for this reaction.[24] The key role played by the relative arrangement of reactants at the transition state is suggested by the observation that the catalytic ability of alcohol dehydrogenases is highly sensitive to the correct alignment of the reactants within their active sites.[25] Theoretical calculations on the transition states for the gas-phase[26] and for the enzymatic reaction[27] show that the carbonyl group being reduced lies above the dihydropyridine ring at approximately 2.7 Å from C(4) (Scheme 1). Interaction of the carbonyl oxygen atom with either a Zn(II) or a protonated histidine (BH in Scheme 1) is crucial for transition state stabilization in the enzymatic reaction.

Transition State Analog Design

The *N*-oxide group has been used as a transition state analog of a polarized carbonyl moiety in raising antibodies capable of catalyzing an enantioselective reduction of ketones with cyanoborohydride,[28] a reaction akin to the hydride transfer process with dihydropyridines. We reasoned that transition state analogs for the hydride transfer process should consist of an *N*-oxide held at an appropriate distance above a mimic of the dihydropyridine ring. A transition state analog for the reduction of acetone by a dihydronicotinamide can be formulated as an *N,N*-dimethyl *N*-oxide bound as benzylic substituents to *ortho*-toluamide, the latter serving as a dihydronicotinamide mimic, giving the hypothetical transition state analog **A**. The transition state C(4)–C(carbonyl) distance of approximately 2.7 Å reported for the calculated transition state[26,27] is accurately mimicked by a 2.59 Å separation between C(2) and the nitrogen atom of the *N*-oxide in this arrangement. That the dihydropyridine in the chemical reaction may be replaced with an aromatic ring in transition state analog **A** is suggested by the fact that dihydropyridines are essentially planar and are isosteric with a benzene ring in their ground state.[29] This replacement was also suggested by the fact that alcohol dehydrogenases are known to stabilize the neutral, reduced form of the NAD cofactor within their active site during hydride transfer.[30]

Due to the absence of cyclic constraints, the relative position of the benzene ring and the *N*-oxide function in transition state analog **A** depends on the values of the dihedral angles θ [C(1)–C(2)–C(methylene)–N] and φ [C(2)–C(methylene)–N–O], which are two freely rotating axes. The desired transition state geometry can only be approached if the dihedral angle θ [C(1)–C(2)–C(methylene)–N] between the benzylic bond and the plane of the aromatic ring is close to 90°. Molecular modelling suggests that the energetically most favorable conformations for **A** do indeed have such a value of θ. Although **A** adopts satisfactory transition state like conformations in modelling experiments, the rotation about θ is almost unhindered.

A greater degree of conformational control, leading to the desired geometries, can be enforced by restricting accessible values of the dihedral angle θ by introducing atropisomerism. Due to the known atropisomerism of naphthalene derivatives, the 2-naphthoic acid derivative **1**, as well as its close relative **2** and **3**, can be expected to exist as separate atropisomers with the dihedral angle θ [C(2)–C(1)–C(methylene)–N] held close to 90°. These compounds adequately mimic the transition state for hydride transfer between acetone and dihydroquinoline cofactors **4–6** (Scheme 2).[31] The *N*-oxide group might adopt a variety of orientations by rotation about φ [C(2)–C(methylene)–N–O]. In the transition state, a similar degree of rotational freedom exists for rotation about the H–C(carbonyl) axis (φ′) and calculations suggest that, in enzyme active sites, this parameter is dictated by the interaction with the activating group Zn(II) or BH.[27]

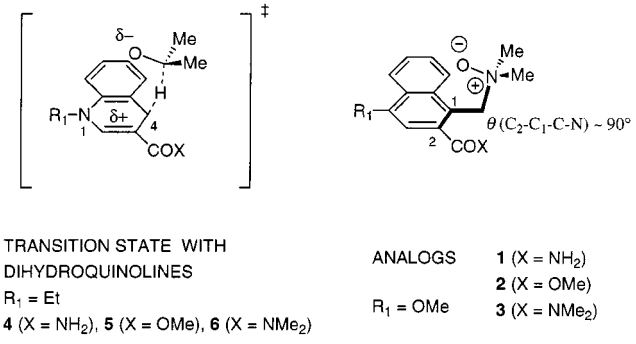

Scheme 2. Transition state of hydride transfer between dihydroquinolines and acetone and atropisomeric transition state analogs

Synthesis

Naphthoic ester **7** was prepared from acetophenone and diethyl succinate using known procedures and then brominated to give bromide **8** (Scheme 3).[32]

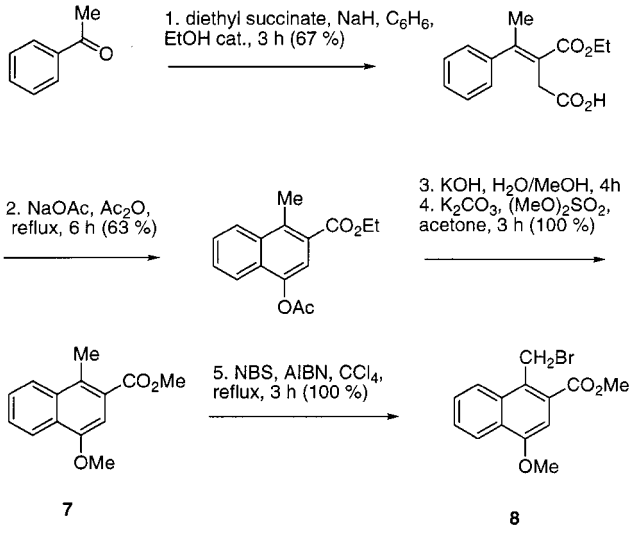

Scheme 3. Synthesis of intermediate **8**[32]

Selective aminolysis of bromide **8** with dimethylamine gave **9**. Aminolysis of **9** with ammonia or with further dimethylamine gave **10** and **11**, respectively. Oxidation of **9**, **10**, and **11** with *m*-CPBA gave **2**, **1**, and **3** (Scheme 4).

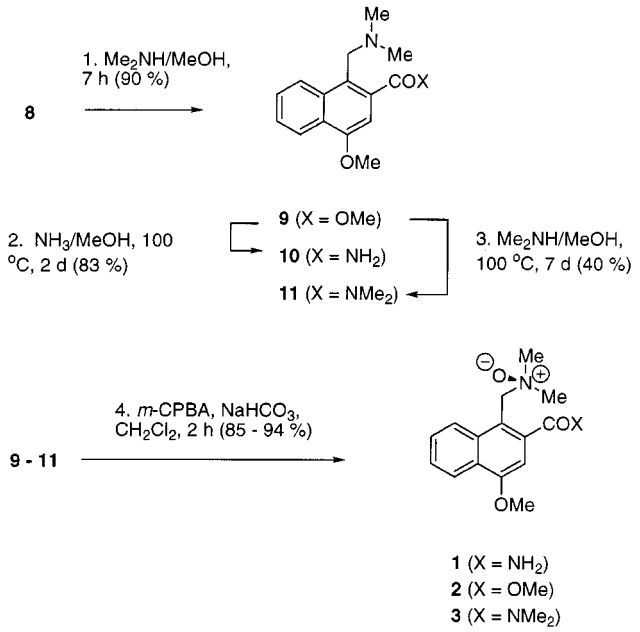

Scheme 4. Synthesis of model transition state analogs

Structure and Atropisomerism

Compound **2** was crystallized and its structure was determined by X-ray crystallography. As expected, the benzylic *N*-oxide substituent lies above the plane of the naphthalene ring, with θ [C(2)–C(1)–C(methylene)–N] = 75°, showing a slight tilt towards the carbomethoxy group. For comparison purposes, we generated a model of the transition state for hydride transfer between acetone and dihydroquinoline cofactor **5** (Figure 1). Distance and angular data reported for the formate dehydrogenase reaction[27c] were used to place the carbonyl group of the substrate at the appropriate distance and angle in relation to the quinoline ring.

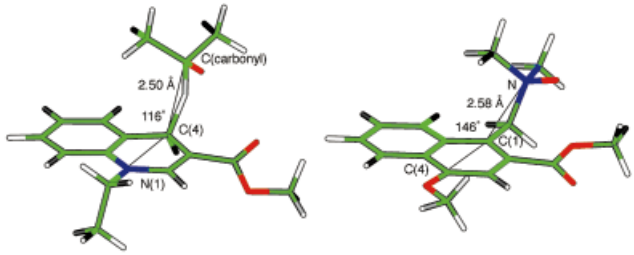

Figure 1. Model for transfer hydride transition state between dihydroquinoline **5** and acetone (left) and structure of analog **2** according to X-ray structure data (right); tube models with N(1)–C(4)–C(carbonyl) resp. C(4)–C(1)–N angles in degrees and the C(4)–C(carbonyl) and C(1)–N distance in Å

As discussed above, the value of the dihedral angle ϕ′ for rotation about the H–C(carbonyl) axis in the transition state of the enzymatic hydride transfer process (Scheme 1) is dictated by interaction with a BH residue on the enzyme. Similarly, in a catalytic antibody raised against a conformer of our transition state analog with a given angle ϕ [C(2)–C(methylene)–N–O], the hydride transfer transition state would be forced to adopt the corresponding value of the dihedral angle ϕ′, probably through interaction with a BH residue on the antibody that would have been induced by the *N*-oxide function of the transition state analog in the course of immunization. To achieve such a situation in our comparison, the carbonyl group in the transition state can be oriented about ϕ to fit the observed orientation of the *N*-oxide in transition state analog **2**. Finally, the carboxyl group of the naphthalene cofactor **5** is oriented with a 20° out-of-plane tilt to fit the accepted model for hydride transfers with such cofactors.[27]

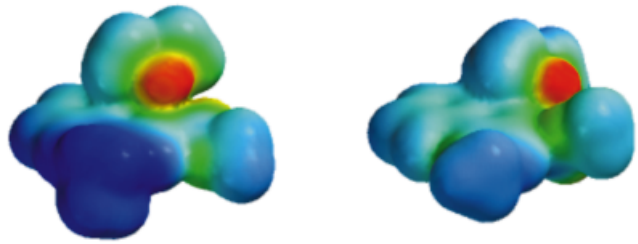

Figure 2. Electron density surface colored with electrostatic potential for model transition state (left) and transition state analog **2** (right); surface coloration goes from red (most negative) to blue (most positive), set at the same values for both structures; the surface was calculated at semiempirical level using the PM3 model as implemented in SPARTAN v5 from Wavefunction, Inc. Irvine (CA), USA

The similarity between the transition state model and the analog can be appreciated by inspection of Figure 1 and 2. The carbonyl group of the substrate, placed at 2.50 Å from C(4) of dihydropyridine **5** at an angle of 116°, is mimicked by the *N*-oxide group in **2**, which is located at 2.58 Å from C(1) at an angle of 146°. The electrostatic potential surfaces compare well; in particular, the *N*-oxide group is an excel-

lent mimic for the polarized carbonyl group undergoing reduction. A noticeable discrepancy between the transition state and the analog concerns the orientation of the carboxyl substituent of the dihydroquinoline. It has been shown for dihydronicotinamide that at the transition state the carboxamide group is tilted out of the plane of the molecule by approximately 20°, with the C=O moiety pointing towards the carbonyl compound being reduced. The same effect is believed to govern stereoselectivity of hydride transfer with chiral dihydropyridines[33,34] and dihydroquinolines,[35] and also occurs with other substituents at the carboxyl groups. This 20° out-of-plane tilt is not correctly mimicked by analog **2**, where the carboxymethyl substituent is tilted out of the plane by –40°, away from the reduction direction. A systematic conformational search by molecular modelling showed that this unfavorable orientation is indeed the most stable orientation and not an effect of crystal packing. The same effect is predicted for compounds **1** and **3**. Interestingly, an intramolecular H-bond, leading to a correct orientation of the carboxyl group with regard to transition state mimicry, is observed in the crystal structure of amino acid **12** (Figure 3), which was obtained in crystalline form following hydrolysis of **9**.

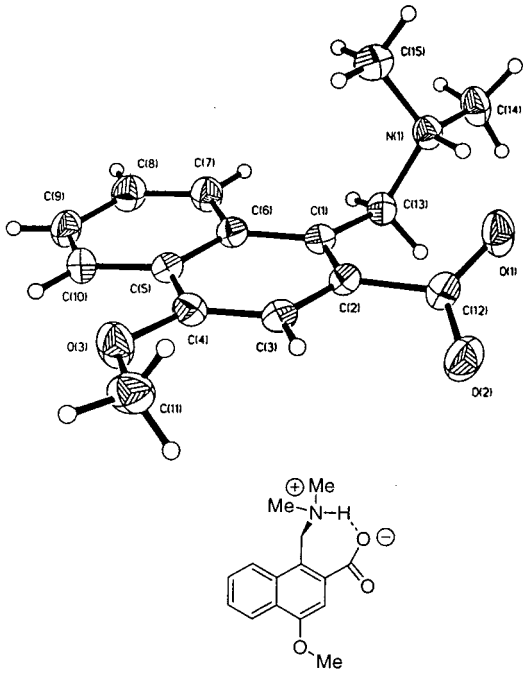

Figure 3. Amino acid **12** and X-ray strucure; the carboxyl group is tilted by 28.2° relative to the aromatic plane due to the intramolecular H bond

In order to determine whether enantiomeric forms of **1**–**3** actually exist as atropisomers, their conformational stabilities in solution were investigated by NMR spectroscopy.[36] ^{1}H- and ^{13}C-NMR spectra were recorded in methanol solution at various temperatures. In all cases, characteristic line broadening and signal splitting was observed for the benzylic methylene proton resonances. This signal would only appear as a singlet at high temperature if free rotation of the methylene group and its *N*-oxide substituent about the C(1)–C(methylene) bond were to be possible; its splitting into an AB system indicates that this rotation is frozen at lower temperatures. Signal splitting is observed for the methyl substituents of the *N*-oxide, which would also be expected on freezing the rotation about the C(1)–C(methylene) bond. The activation energy for this rotation can be calculated from the NMR data (Table 1 and Figure 4).[37] These results show that enantiomers of **1**–**3** exist as separate atropisomers on the NMR time scale. In contrast, the ^{1}H- and ^{13}C-NMR signals for **12** and its methyl ester **9** do not show any splitting, even at low temperatures, suggesting that in these compounds the dimethylamino group rotates more rapidly than the observable NMR time scale.

Table 1. Atropisomerism of compounds **1–3** as measured by variable-temperature ^{1}H-NMR; spectra were recorded in CD_3OD at 10 K intervals between 223 K and 323 K

Compound	Signal	T_c (°C)[a]	ΔG (kJmol^{-1})[b]	$k_{coal.}$ (s^{-1})[c]
1	$N(CH_3)_2$	30	61	184
	Ar–CH_2–N	40	63	101
2	$N(CH_3)_2$	20	56	431
	Ar–CH_2–N	20	54	324
3	$N(CH_3)_2$	25	59	314
	Ar–CH_2–N	50	62	674

[a] Temperature by which coalescence of ^{1}H NMR signals is observed. – [b] Calculated activation energy for equilibration of atropisomers: $\Delta G = RT_c(22.96 + \ln(T_c/\delta\gamma))$ (methyl signals) and $\Delta G = RT_c(23.76 - \ln(k_{coal.}/T_c))$ (methylene signals). – [c] Rate of equlibration at coalescence temperature. $k_{coal.} = 2.22\delta\gamma$ (methyl signals) and $k_{coal.} = \pi(\delta\gamma^2 + 6J^2_{AB})/1.414$ (methylene signals).

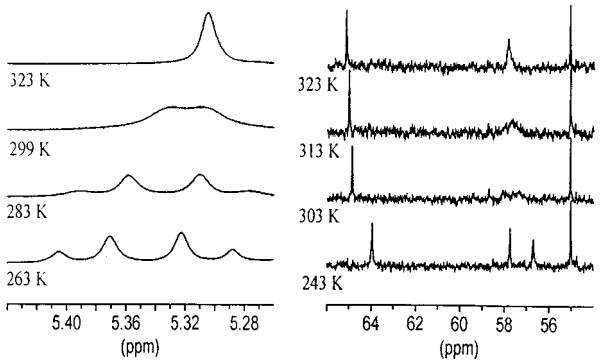

Figure 4. NMR signal splittings; ^{1}H-NMR methylene signals for compound **1** (left) and ^{13}C-NMR methylene signal for compound **2** (right) at representative temperatures

The height of the rotational barrier evaluated from the NMR data is approximately 50–60 kJmol^{-1} for all three compounds. The nature of the carboxyl substituent on the naphthalene ring has relatively little influence on the rate of equilibration between atropisomers, which suggests that isomerization might occur by rotation on the side of the aromatic group ($\theta = 180°$) rather than on the side of the carboxyl group ($\theta = 0°$). To test these hypotheses, we carried out semiempirical calculations on **1**–**3**. In all three cases, rotation about the C(1)–C(methylene) bond was predicted to have a lower activation energy for rotation on the side of the aromatic group, amounting to approximately 56 kJmol^{-1} for **1**, 50 kJmol^{-1} for **2**, and 45 kJmol^{-1} for **3** (Fig-

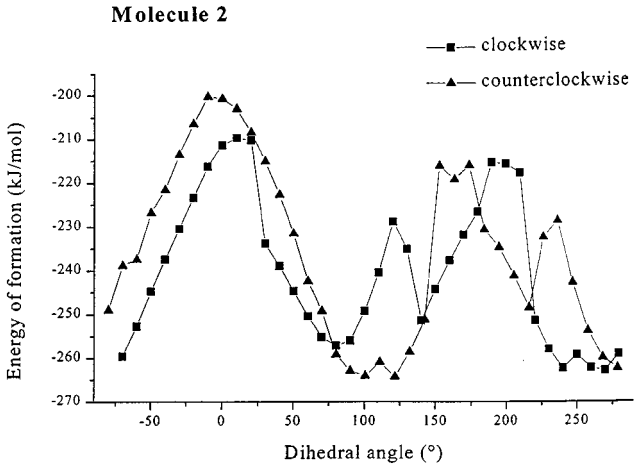

Figure 5. Simulated energy profile for atropisomerization of compound **2**; the calculated heats of formation are plotted against the constrained dihedral angle θ = C(2)–C(1)–C(methylene)–N; the starting structure was constructed using the X-ray coordinates of molecule **2**, followed by geometry optimization; from the obtained, energy-minimized structures, the rotation barrier around the C(1)–C(methylene) bond was analysed using the coordinate driving procedure of SPARTAN: the dihedral angle was constrained in 10° increments until a complete rotation was achieved, both clockwise and counterclockwise; each constrained structure was fully energy-minimized before incrementing the dihedral angle; similar procedures were carried out for compounds **1** and **3** (data not shown); all calculations were performed at the semiempirical level using the PM3 model as implemented in SPARTAN v5 from Wavefunction, Inc., Irvine (CA), USA; the geometry of each structure was pre-optimized using the SYBYL forcefield

ure 5). It must be pointed out that the starting conformation in these calculations is chiral, so that clockwise and counterclockwise rotations are diastereoisomeric and not superimposable. These calculations nicely support our NMR measurements.

These measurements demonstrate that, in spite of rapid equilibration, only atropisomeric conformers with the *N*-oxide placed above the naphthalene ring, corresponding to the geometry of the hydride transfer process to be mimicked, are significantly populated in solution. The binding energies associated with non-covalent interactions of transition state analogs with their typical target proteins, either an enzyme if they are used as inhibitors or an antibody if they are used as immunogenic haptens in the context of an immunization experiment, are typically of the order of 10–20 kcal/mol. Within this energy range, the energetic handicap associated with recognition of a conformer less stable than the most stable conformer by only a few kcal/mol would be prohibitive. Here, recognition of unstable "in plane" conformers of compounds **1–3** would be associated with a 15 kcal/mol handicap for binding. In the context of immunization experiments, the most stable conformers are also the most populated, and will thus be most frequently encountered by the immune system. Therefore, we believe that our design principle may be exploited in the context of transition state analogs despite the fact that the atropisomeric forms of our compounds are not separable. In the context of an immunization experiment, the molecules could be linked to a carrier protein by means of an alkyl chain attached to one of the methyl substituents of the amine oxide function, thereby mimicking the transition state of the reaction of an alkyl methyl ketone.

Conclusion

We have shown that atropisomerism can be exploited in the design of conformationally stable transition state analogs. In the example presented here, restricted rotation allows the positioning of an *N*-oxide above a naphthalene ring to serve as a mimic for a polarized carbonyl group in a hydride transfer process. The almost exact match of the C(4)–C(carbonyl) distance of 2.7 Å in the transition state by the C(1)–N distance of 2.59 Å in our analogs is noteworthy. Indeed, it is often almost impossible to design analogs displaying accurate transition state distances. As discussed above, the fact that atropisomers may not be separable due to rapid equilibration is probably not a handicap in the context of transition state analogs. The rotational barriers of approximately 15 kcal/mol measured here are sufficient to ensure that only the more stable conformers displaying the correct transition state geometry will be significantly populated in solution and thus recognized in a non-covalent binding interaction with a target protein. This design should be applicable to processes involving similar transition state geometries, such as the aldol reaction[38] and aromatic substitution reactions.

Experimental Section

General: Reagents were purchased from Aldrich or Fluka. – All chromatography (flash) was performed on Merck silica gel 60 (0.040–0.063 mm). – Preparative HPLC was carried out with Fisher Optima grade acetonitrile and ordinary deionized water using a Waters prepak cartridge 500 g installed on a Waters Prep LC 4000 system from Millipore, flow rate 100 mL/min., gradient + 0.5%/min CH_3CN; detection by UV at 254 nm. – TLC was performed on fluorescent F254 glass-backed plates. – NMR spectra were recorded with Bruker AM-250 (250 MHz) or AM-300 (300 MHz) instruments. – IR spectra were recorded with a Perkin–Elmer 1600 Series FT-IR instrument. – Melting points were determined with a Büchi 510 melting point apparatus. – MS and HRMS data were provided by Analytical Research Services (Dr. T. Schürch, University of Bern) and by the Scripps Research Institute MS facility (Dr. G. Siuzdak). The procedure for the synthesis of compound **7** was carried out in accordance with the original literature[32] without significant changes, as detailed below.

Ethyl 4-Acetoxy-1-methyl-2-naphthoate: 3-Ethyloxycarbonyl-4-phenyl-3-pentenoic acid, obtained from acetophenone and diethyl succinate, was refluxed for 12 h in acetic anhydride (90 mL, 95 mmol) containing sodium acetate (9.00 g, 100 mmol). The excess acetic anhydride was then removed by co-evaporation with toluene and the dark-brown residue was treated with iced water (300 mL) and extracted with diethyl ether (3 × 250 mL). The combined ethereal extracts were washed with satd. aq. Na_2CO_3 solution (100 mL), dried (Na_2SO_4), and the solvent was evaporated. Chromatography

(hexane/ethyl acetate, 10:1) of the residue gave ethyl 4-acetoxy-1-methyl-2-naphthoate (8.3 g, 63%) as a colorless solid. TLC (hexane/ethyl acetate, 10:3): R_f (starting materials) = 0.43 and 0.37, R_f (product) = 0.57. – ^{1}H NMR (250 MHz, $CDCl_3$): δ = 8.22 (m, 1 H), 7.85 (m, 1 H), 7.68–7.53 (m, 3 H), 4.42 (q, J = 7.1 Hz), 2.91 (s, 3 H), 2.49 (s, 3 H), 1.43 (t, J = 7.1 Hz). – ^{13}C NMR (65.5 MHz, $CDCl_3$): δ = 169.4, 167.0, 145.2, 135.5, 133.9, 127.8, 126.9, 125.6, 121.4, 118.2, 61.1, 20.9, 15.6, 14.2. – HRMS: $C_{16}H_{16}NO_4^+$ [M + H^+]: calcd. 272.1049; found 272.1042.

4-Hydroxy-1-methyl-2-naphthoic Acid: Ethyl 4-acetoxy-1-methyl-2-naphthoate (3.3 g, 12 mmol) was dissolved in aqueous KOH (30%, 30 mL) and methanol (30 mL) and the resulting mixture was heated under reflux for 4 h. The mixture was then cooled to 20 °C, diluted with water (100 mL), and washed with CH_2Cl_2 (2 × 100 mL). The aqueous phase was acidified with 6 N HCl and extracted with diethyl ether (2 × 100 mL) to give 4-hydroxy-1-methyl-2-naphthoic acid in quantitative yield (2.50 g) as a white crystalline solid. – TLC ($CHCl_3$/AcOH, 20:1): R_f (starting material) = 0.70, R_f (product) = 0.15. – ^{1}H NMR (250 MHz, CD_3OD): δ = 8.08 (m, 1 H), 7.85 (m, 1 H), 7.37–7.22 (m, 2 H), 6.92 (s, 1 H), 4.90 (br. s, 1 H), 2.56 (s, 3 H). – ^{13}C NMR (65.5 MHz, CD_3OD): δ = 172.8, 152.5, 135.2, 129.9, 127.9, 127.7, 127.0, 126.0, 123.5, 15.4. – HRMS: $C_{12}H_{10}O_3^+$ [M + H^+]: calcd. 202.0630; found 202.0626.

Methyl 4-Methoxy-1-methyl-2-naphthoate (7): A mixture of 4-hydroxy-1-methyl-2-naphthoic acid (1.12 g, 5.55 mmol), dry K_2CO_3 (6.88 g, 49.78 mmol), and dimethyl sulfate (4.47 g, 35.44 mmol) in anhydrous acetone (41.4 mL) was heated for 4 h under reflux. The mixture was then allowed to cool to room temperature, water (130 mL) was added, and the acetone was removed in vacuo. The remaining aqueous phase was then extracted with diethyl ether (2 × 200 mL), the combined extracts were dried over sodium sulfate, and the solvent was evaporated to yield **7** as a colorless solid (1.27 g, 100%). – TLC (hexane/ethyl acetate, 10:3): R_f = 0.41. – ^{1}H NMR (250 MHz, $CDCl_3$): δ = 8.31 (m, 1 H), 8.11 (m, 1 H), 7.62–7.50 (m, 2 H), 7.12 (s, 1 H), 4.05 (s, 3 H), 3.88 (s, 3 H). – ^{13}C NMR (65.5 MHz, $CDCl_3$): δ = 169.3, 153.3, 133.6, 129.0, 127.4, 127.0, 126.9, 126.6, 125.1, 122.2, 103.4, 55.4, 52.1, 15.3. – IR ($CHCl_3$): $\tilde{\nu}$ = 3410, 3018, 2962, 2646, 2476, 1636, 1472, 1398, 1038 cm^{-1}. – HRMS: $C_{14}H_{14}O_3^+$ [M + H^+]: calcd. 230.0943; found 230.0928.

Methyl 1-(Bromomethyl)-4-methoxy-2-naphthoate (8): Methyl 4-methoxy-1-methyl-2-naphthoate (**7**) (2.00 g, 8.69 mmol), *N*-bromosuccinimide (1.85 g, 10.4 mmol), and azobis(isobutyronitrile) (20 mg) were suspended in CCl_4 (70 mL) and the mixture was heated to reflux. The reaction was monitored by TLC (hexane/ethyl acetate, 10:3) and terminated once all the starting material (R_f = 0.7) had been consumed (105 min.). The mixture was then cooled to 20 °C and the solids were filtered off and washed with CCl_4 (2 × 15 mL). Concentration of the combined organic phases yielded **8** in quantitative yield (2.70 g) as a slightly yellow solid. This bromide (R_f = 0.6) was used for the next step without further purification. – ^{1}H NMR (250 MHz, $CDCl_3$): δ = 8.33–8.21 (m, 2 H), 7.69–7.57 (m, 2 H), 7.15 (s, 1 H), 5.39 (s, 2 H), 4.03 (s, 3 H), 3.88 (s, 3 H). – ^{13}C NMR (65.5 MHz, $CDCl_3$): δ = 155.7, 132.3, 127.8, 127.3, 124.7, 122.2, 103.9, 55.7, 52.6, 27.3.

Methyl 1-(Dimethylamino)methyl-4-methoxy-2-naphthoate (9): A solution of bromide **8** (1.50 g, 4.85 mmol) in 80 mL of anhydrous methanol saturated with dimethylamine (5.6 M) was stirred for 5 h at 20 °C. Evaporation of the solvent and chromatography (hexane/CH_2Cl_2/acetone, 80:80:1) of the residue yielded **9** as a colorless product (1.19 g, 90%). – TLC (1. hexane/ethyl acetate, 10:2 + 0.5 NEt_3; 2. hexane/ethyl acetate, 10:2): R_f = 0.33. – ^{1}H NMR (250 MHz, $CDCl_3$): δ = 8.38–8.22 (m, 2 H), 7.62–7.48 (m, 2 H), 6.97 (s, 1 H), 4.02 (s, 1 H), 3.97 (s, 3 H), 3.91 (s, 3 H), 2.25 (s, 6 H). – ^{13}C NMR (65.5 MHz, $CDCl_3$): δ = 170.1, 154.5, 133.4, 130.2, 127.8, 127.1, 126.7, 126.3, 125.4, 122.1, 102.8, 55.9, 55.5, 52.1, 45.1, 29.5. – IR ($CHCl_3$): $\tilde{\nu}$ = 2948, 2674, 2490, 1472, 1398, 1036 cm^{-1}. – FAB-MS: m/z = 296 [M + Na^+], 274 [M + H^+].

1-(Dimethylamino)methyl-4-methoxy-2-naphthoamide (10): A solution of compound **9** (140 mg, 0.51 mmol) in 17 mL of NH_3/MeOH (8.3 M) was stirred at 100 °C for 3 d. Evaporation of the solvent and chromatography (CH_2Cl_2/CH_3OH, 10:1) of the residue gave **10** (110 mg, 83%) as a colorless solid. – TLC (CH_2Cl_2/methanol, 10:2): R_f (**9**) = 0.47, R_f (**10**) = 0.28. – ^{1}H NMR (250 MHz, $CDCl_3$/CD_3OD): δ = 8.22–8.13 (m, 2 H), 7.51–7.42 (m, 2 H), 7.04 (s, 1 H), 4.06 (s, 2 H), 3.51 (s, 1 H), 2.68 (s, 1 H), 2.34 (s, 6 H). – ^{13}C NMR (65.5 MHz, $CDCl_3$/CD_3OD): δ = 172.5, 155.1, 135.2, 133.1, 127.8, 127.1, 126.3, 126.0, 125.9, 123.9, 122.4, 103.1, 54.9, 54.0, 42.7. – MS (electrospray$^+$): m/z = 517 [2M + H^+], 259 [M + H^+].

***N*-[(2-Carbamoyl-4-methoxy-1-naphthyl)methyl]-*N,N*-dimethylamine Oxide (1):** Compound **10** (105 mg, 0.41 mmol), *m*-CPBA (189 mg, 0.82 mmol), and Na_2CO_3 (200 mg) were suspended in 5 mL of CH_2Cl_2/MeOH, 1:1, and the mixture was stirred at 20 °C for 2.5 h, after which the reaction was complete. The mixture was then filtered and the residue was washed with CH_2Cl_2/MeOH, 4:1 (2 × 10 mL). Evaporation of the solvents and chromatography (CH_2Cl_2/MeOH, 10:1) of the residue gave 95 mg (85%) of **1** as an oily product. – ^{1}H NMR (300 MHz, CD_3OD): δ = 7.92–7.80 (m, 2 H), 7.65–7.02 (m, 2 H), 7.22 (s, 1 H), 5.38 (br. s, 2 H), 4.16 (s, 3 H), 3.43–3.17 (br. s, 6 H). – ^{13}C NMR (72.5 MHz, CD_3OD): δ = 174.5, 158.0, 140.6, 135.2, 128.8, 127.5, 127.3, 126.5, 123.4, 116.3, 104.9, 66.1, 59.4 (br.), 58.9 (br.), 56.3. – HRMS: $C_{15}H_{18}N_2O_3^+$ [M + H^+]: calcd. 275.1396; found 275.1405.

***N*-[(4-Methoxy-2-methoxycarbonyl-1-naphthyl)methyl]-*N,N*-dimethylamine Oxide (2):** A similar procedure as described above, but using neat dichloromethane (6 mL) and starting with compound **9** (130 mg, 0.4756 mmol), yielded 130 mg (94%) of **2** as a colorless solid; m.p. 132–133 °C. – TLC (CH_2Cl_2/methanol, 10:2): R_f (**9**) = 0.28, R_f (**2**) = 0.39. – ^{1}H NMR (300 MHz, CD_3OD): δ = 8.32 (d, J = 8.5 Hz, 1 H), 8.18 (d, J = 8.5 Hz, 1 H), 7.56–7.43 (m, 2 H), 7.14 (s, 1 H), 5.20 (br. s, 2 H), 3.93 (s, 3 H), 3.85 (s, 3 H), 3.08–2.85 (br. s, 6 H). – ^{13}C NMR (72.5 MHz, CD_3OD): δ = 173.2, 160.4, 138.5, 138.2, 131.7, 130.5, 130.4, 129.2, 126.0, 122.3, 107.7, 67.4, 61.2, 58.9, 55.7. – IR ($CHCl_3$): $\tilde{\nu}$ = 3020, 2928, 2400, 1752, 1590, 1464, 1370, 1106 cm^{-1}. – HRMS: $C_{16}H_{30}NO_4^+$ [M + H^+]: calcd. 290.139280; found 290.139233.

***N*-{[2-(*N′,N′*-Dimethylcarbamoyl)-4-methoxy-1-naphthyl]methyl}-*N,N*-dimethylamine Oxide (3):** A solution of compound **9** (210 mg, 0.77 mmol) in 15 mL of 5.6 M dimethylamine in methanol containing sodium cyanide (50 mg, cat.) was stirred for 7 d at 100 °C. Evaporation of the solvent, work-up (aq. $NaHCO_3$/CH_2Cl_2), and chromatography (hexane/CH_2Cl_2/acetone, 80:80:1) of the residue gave **11** as a colorless solid (90 mg, 40%). – TLC (hexane/ethyl acetate, 10:3): R_f (**9**) = 0.22, R_f (**11**) = 0.11. Amine **11** (37 mg, 0.1292 mmol) was further oxidized with *m*-CPBA in 5 mL of CH_2Cl_2 as described above. After 1 h, work-up and subsequent chromatography (CH_2Cl_2/MeOH, 10:1) and preparative reversed-phase HPLC gave 35 mg (90%) of **3** as an oily product. – TLC (CH_2Cl_2/methanol, 10:2): R_f (**11**) = 0.55, R_f (**3**) = 0.11. – ^{1}H NMR (300 MHz, CD_3OD, 296 K): δ = 8.43–8.33 (m, 2 H), 7.79–7.64 (m, 2 H), 7.06 (s, 1 H), 5.66 (br. s, 2 H), 4.10 (s, 3 H), 3.53–3.29 (br. s,

6 H), 3.23 (s, 3 H), 2.95 (s, 3 H). – ^{13}C NMR (72.5 MHz, CD_3OD, 296 K): δ = 129.7, 128.9, 127.7, 127.2, 125.9, 125.8, 122.1, 59.2 (br.), 56.5 (br.), 55.2, 34.0. – IR ($CHCl_3$): $\tilde{\nu}$ = 3452, 3010, 2421, 1684, 1628, 1594, 1464, 1416, 1200 cm^{-1}. – MS (EI-MS): *m/z* = 257 [M – 45], 241 [M – 61], 227 [M – 75], 212 [M – 90].

1-[(Dimethylamino)methyl]-4-methoxy-2-naphthoic Acid (12): An analytical sample of methyl ester **9** was dissolved in 2-propanol/dichloromethane/aq. ammonia (10:10:1) for crystallization purposes. Under these conditions, the methyl ester was cleaved and crystals of compound **12** could be collected after 3 days at 20 °C; m.p. 224–226 °C (dec.). – ^{1}H NMR (250 MHz, CD_3OD): δ = 8.32–8.28 (m, 2 H), 7.72–7.53 (m, 2 H), 7.39 (s, 1 H), 4.69 (s, 2 H), 4.08 (s, 3 H), 2.83 (s, 6 H). – ^{13}C NMR (65.5 MHz, $CDCl_3$): δ = 173.2, 156.6, 133.5, 128.4, 127.5, 127.1, 126.7, 123.8, 123.4, 118.7, 107.1, 56.5, 55.1, 42.2. – HRMS: $C_{15}H_{17}NO_3^+$ [M + H^+]: calcd. 259.1208; found 259.1189.

Crystallographic Data: Crystallographic data (excluding structure factors) for the structures of **2** and **12** have been deposited with the Cambridge Crystallographic Data Centre as supplementary publication nos. CCDC-125392 (**2**) and CCDC-121427 (**12**). Copies of the data can be obtained free of charge on application to the CCDC, 12 Union Road, Cambridge CB2 1EZ, U.K. [Fax: (internat.) +44 (0)1223/336033; E-mail: deposit@ccdc.cam.ac.uk].

Acknowledgments

We thank Dr. R. A. Lerner for his support and Dr. T. Ward for helpful suggestions. Financial support for this work was provided by the Deutsche Forschungsgemeinschaft and the Roche Foundation (postdoctoral fellowships to O. R.), the Swiss National Science Foundation, the Koordinationsgruppe für Forschungsfragen der Basler chemischen Industrie (KGF), and the Wander Stiftung.

[1] J. Kraut, *Science* **1988**, *242*, 533 and refs. cited therein.
[2] [2a] J. L. Kurz, *Acc. Chem. Res.* **1972**, *5*, 1–9. – [2b] O. S. Tee, *Adv. Phys. Org. Chem.* **1994**, *29*, 1–85. – [2c] R. Wolfenden, *Acc. Chem. Res.* **1972**, *5*, 10–18. – [2d] G. E. Lienhard, *Science* **1973**, *180*, 149–154. – [2e] J.-L. Reymond, Y. Chen, *Isr. J. Chem.* **1996**, *36*, 199–206.
[3] [3a] M. M. Mader, P. A. Bartlett, *Chem. Rev.* **1997**, *97*, 1281–1301. – [3b] J. D. Stewart, S. J. Benkovic, *Nature* **1995**, *375*, 388–391. – [3c] A. J. Kirby, *Angew. Chem.* **1996**, *108*, 771–790; *Angew. Chem. Int. Ed. Engl.* **1996**, *35*, 707–724. – [3d] I. Fujii, F. Tanaka, H. Miyashita, R. Tanimura, K. Kinoshita, *J. Am. Chem. Soc.* **1995**, *117*, 6199–6209.
[4] [4a] P. G. Schultz, R. A. Lerner, *Science* **1995**, *269*, 1835–1842. – [4b] J.-L. Reymond, *Top. Curr. Chem.* **1999**, *200*, 59–93.
[5] H. Primas, U. Müller-Herold in *Elementare Quantenchemie*, 2. Aufl./2nd Ed., Teubner, Stuttgart, **1990**, p. 189–190.
[6] Compound types other than transition state analogs can be utilized to prepare enzyme inhibitors and/or haptens inducing catalytic antibodies. Examples include suicide inhibitors, bait and switch, and reactive immunizations.
[7] M. Bols, *Acc. Chem. Res.* **1998**, *31*, 1–8 and refs. cited therein.
[8] [8a] L. J. Liotta, R. A. Gibbs, S. D. Taylor, P. A. Benkovic, S. J. Benkovic, *J. Am. Chem. Soc.* **1995**, *117*, 4729–4741. – [8b] O. Ersoy, R. Fleck, A. Sinskey, S. Masamune, *J. Am. Chem. Soc.* **1996**, *118*, 13077–13078.
[9] [9a] K. D. Janda, C. G. Shevlin, R. A. Lerner, *Science* **1993**, *259*, 490–493. – [9b] K. D. Janda, C. G. Shevlin, R. A. Lerner, *J. Am. Chem. Soc.* **1995**, *117*, 2659–2560.
[10] [10a] T. Li, K. D. Janda, J. A. Ashley, R. A. Lerner, *Science* **1994**, *264*, 1289–1293. – [10b] T. Li, S. Hilton, K. D. Janda, *J. Am. Chem. Soc.* **1995**, *117*, 3308–3309. – [10c] T. Li, K. D. Janda, R. A. Lerner, *Nature* **1996**, *379*, 326–327. – [10d] J. Hasserodt, K. D. Janda, R. A. Lerner, *J. Am. Chem. Soc.* **1996**, *118*, 11654–11655 and **1997**, *119*, 5993–5998. – [10e] J. Hasserodt, K. D. Janda, *Tetrahedron* **1997**, *53*, 11237–11255.
[11] A. C. Braisted, P. G. Schultz, *J. Am. Chem. Soc.* **1994**, *116*, 2211–2212.
[12] Z. S. Zhou, N. Jiang, D. Hilvert, *J. Am. Chem. Soc.* **1997**, *119*, 3623–3624.
[13] S. S. Yoon, Y. Oei, E. Sweet, P. G. Schultz, *J. Am. Chem. Soc.* **1996**, *118*, 11686–11687.
[14] D. Y. Jackson, P. G. Schultz, *J. Am. Chem. Soc.* **1991**, *113*, 2319–2320.
[15] T. Uno, J. Ku, J. R. Prudent, A. Huang, P. G. Schultz, *J. Am. Chem. Soc.* **1996**, *118*, 3811–3817.
[16] [16a] P. A. Bartlett, C. R. Johnson, *J. Am. Chem. Soc.* **1985**, *107*, 7792–7793. – [16b] D. Y. Jackson, J. W. Jacobs, R. Sugasawara, S. H. Reich, P. A. Bartlett, P. G. Schultz, *J. Am. Chem. Soc.* **1988**, *110*, 4841–4842. – [16c] M. R. Haynes, E. A. Stura, D. Hilvert, I. A. Wilson, *Science* **1994**, *263*, 646–652.
[17] [17a] D. Hilvert, K. W. Hill, K. D. Nared, M.-R. M. Auditor, *J. Am. Chem. Soc.* **1989**, *111*, 9261–9262. – [17b] A. C. Braisted, P. G. Schultz, *J. Am. Chem. Soc.* **1990**, *112*, 7430–7431. – [17c] V. E. Gouverneur, K. N. Houk, B. de Pascual-Teresa, B. Beno, K. D. Janda, R. A. Lerner, *Science* **1993**, *262*, 204–208. – [17d] C. J. Suckling, M. C. Tedford, L. M. Bence, J. I. Irvine, W. H. Stimson, *J. Chem. Soc., Perkin Trans. 1* **1993**, 1925–1929. – [17e] A. A. P. Meekel, M. Resmini, U. K. Pandit, *Bioorg. Med. Chem.* **1996**, *4*, 1051–1057.
[18] B. F. Cravatt, J. A. Ashley, K. D. Janda, D. L. Boger, R. A. Lerner, *J. Am. Chem. Soc.* **1994**, *116*, 6013–6014.
[19] H. Suga, N. Tanimoto, A. J. Sinskey, S. Masamune, *J. Am. Chem. Soc.* **1994**, *116*, 11197–11198.
[20] J. T. Yli-Kauhaluoma, J. A. Ashley, C.-H. Lo, J. Coakley, P. Wirsching, K. D. Janda, *J. Am. Chem. Soc.* **1996**, *118*, 5496–5497.
[21] M. Oki, *Top. Stereochem.* **1983**, *14*, 1–79.
[22] [22a] J. Clayden, *Angew. Chem.* **1997**, *109*, 986–987; *Angew. Chem. Int. Ed. Engl.* **1997**, *36*, 949–951. – [22b] J. Clayden, M. Darbyshire, J. H. Pink, N. Westlund, F. X. Wilson, *Tetrahedron Lett.* **1997**, *38*, 8587–8590.
[23] [23a] M. G. Rossman, A. Liljas, C.-I. Brändén, L. J. Banaszak, "Evolutionary and structural relationship among dehydrogenases", in *The Enzymes*, Academic Press, Inc., **1975**, vol. *11*, p. 61. – [23b] N. J. Oppenheimer, A. L. Handlon, "Mechanism of NAD-dependent enzymes", in *The Enzymes*, Academic Press, Inc., **1992**, vol. *20*, p. 453.
[24] J. Schröer, M. Sanner, J.-L. Reymond, R. A. Lerner, *J. Org. Chem.* **1997**, *62*, 3220–3229.
[25] A. D. Mesecar, B. L. Stoddard, D. E. Koshland, Jr., *Science* **1997**, *277*, 202–206.
[26] [26a] J. W. Verhoeven, W. van Gerresheim, F. M. Martens, S. M. van der Kerk, *Tetrahedron* **1986**, *42*, 975–992. – [26b] Y.-D. Wu, K. N. Houk, *J. Am. Chem. Soc.* **1987**, *109*, 2226–2227. – [26c] O. Tapia, R. Cardenas, F. Colonna-Cesari, *J. Am. Chem. Soc.* **1988**, *110*, 4046–4047. – [26d] J. Wilkie, I. H. Williams, *J. Am. Chem. Soc.* **1992**, *114*, 5423–5425. – [26e] Y.-D. Wu, D. K. W. Lai, K. N. Houk, *J. Am. Chem. Soc.* **1995**, *117*, 4100–4108.
[27] [27a] Ö. Almarsson, R. Karaman, T. C. Bruice, *J. Am. Chem. Soc.* **1992**, *114*, 8702–8703. – [27b] Ö. Almarsson, T. C. Bruice, *J. Am. Chem. Soc.* **1993**, *115*, 2125–2138. – [27c] B. Schiøtt, Y.-J. Zheng, T. C. Bruice, *J. Am. Chem. Soc.* **1998**, *120*, 7192–7200.
[28] L. C. Hsieh, S. Yonkovich, L. Kochersperger, P. G. Schultz, *Science* **1993**, *260*, 337–339.
[29] H.-J. Hofmann, R. Cimiraglia, *FEBS Lett.* **1988**, *241*, 38–40 and refs. cited therein.
[30] K. P. Nambiar, D. M. Stauffer, P. A. Kolodziej, S. A. Benner, *J. Am. Chem. Soc.* **1983**, *105*, 5886–5890.
[31] [31a] A. Ohno, Y. Ishikawa, N. Yamazaki, M. Okamura, Y. Kawai, *J. Am. Chem. Soc.* **1998**, *120*, 1186–1192. – [31b] A. Ohno, Y. Ishihara, S. Ushida, S. Oka, *Tetrahedron Lett.* **1982**, *31*, 3185–3188. – [31c] S. Shinkai, H. Hamada, O. Manabe, *Tetrahedron Lett.* **1979**, 1397–1400.
[32] [32a] S. M. Abdel-Wahhab, L. S. El-Assad, *J. Ind. Chem. Soc.* **1969**, *46*, 927–932. – [32b] O. Muraoka, G. Tanabe, K. Sano, T. Minematsu, *J. Chem. Soc., Perkin Trans. 1* **1994**, 1833–1845.
[33] P. M. T. de Kok, L. A. M. Bastiaansen, P. M. van Lier, J. A. J. M. Vekemans, H. M. Buck, *J. Org. Chem.* **1989**, *54*, 1313–1320.
[34] Recent examples of stereoselective hydride transfer with pyridine cofactors:[34a] N. Kanomata, M. Suzuki, M. Yoshida, T. Nakata, *Angew. Chem.* **1998**, *110*, 1506–1508; *Angew. Chem.*

Int. Ed. Engl. **1998**, *37*, 1410–1412. – [34b] N. Kanomata, T. Nakata, *Angew. Chem.* **1997**, *109*, 1263–1266; *Angew. Chem. Int. Ed. Engl.* **1997**, *36*, 1207–1211. – [34c] S. Obika, T. Nishiyama, S. Tatematsu, K. Miyashita, C. Iwata, T. Imanishi, *Tetrahedron* **1997**, *53*, 593–602. – [34d] T. Eguchi, M. Fukuda, Y. Toyooka, K. Kakinuma, *Tetrahedron* **1998**, *54*, 705–714.

[35] A. Ohno, M. Ohara, S. Oka, *J. Am. Chem. Soc.* **1986**, *108*, 6438–6440.

[36] Related study on naphthylcarbinols: D. Casarini, L. Lunazzi, A. Mazzanti, *J. Org. Chem.* **1997**, *62*, 3315–3323.

[37] H. Günther, *NMR-Spektroskopie*, 3rd ed., Georg Thieme Verlag, Stuttgart, **1992**, pp. 304–322.

[38] J.-L. Reymond, *Angew. Chem.* **1995**, *107*, 2471–2473; *Angew. Chem. Int. Ed. Engl.* **1995**, *34*, 2285–2287.

Received June 28, 1999
[O99387]